UserCom
1/2004

Information for users of METTLER TOLEDO thermal analysis systems

19

**Dear Customer,**
This year METTLER TOLEDO celebrates 40 years of outstanding success in thermal analysis. In 1964 we introduced the TA1, an advanced, research grade TGA/DTA instrument. Since then, we have continuously expanded our TA product line with new ideas and solutions. And now we are proud to introduce the TMA/SDTA841$^e$.
Thermomechanical analysis is more sensitive than DSC for a number of applications. We demonstrated this in UserComs 17 and 18 for the determination of glass transition temperatures. TMA is in fact the ideal complement to a DSC system.

# DSC measurements at high heating rates – advantages and limitations

*Dr. Matthias Wagner, Dr. Rod Bottom, Philippe Larbanois, Dr. Jürgen Schawe*

## Introduction

DSC measurements are usually performed at heating rates of 10 to 20 K/min. This is a good compromise between accuracy, resolution, sensitivity and actual measurement time.

The use of high heating rates represents an attempt to measure the sample in its original state, i.e. so rapidly that the sample has no time to change during the measurement (e.g. cold crystallization).

The recent increased discussion on this topic can be summarized as follows: Measurements at high heating rates lead to

- much shorter experiment times,
- increased sample throughput,
- better sensitivity with certain effects (e.g. the determination of weak glass transitions) because of the greater heat flow signals at higher heating rates and
- less reorganization in the sample during the DSC measurement.

**Contents**

In principle, the software allows high heating rates (up to 400 K/min and more). The accuracy of the results so obtained must be checked with respect to the physical and chemical facts. The laws governing physical and chemical events such as reactions and transitions must be taken into account.

Such events include:
- Heating rate-dependent effects:
  - kinetic events
  - crystallization
  - chemical reactions
  - glass transitions
- Heating rate-independent effects:
  - melting
  - physical properties such as specific heat capacity

Besides this, sample measurement is influenced by the following sample properties and instrument parameters:
Sample
- Situation within the sample:
  - sample size
  - sample homogeneity
  - thermal gradients
  - thermal conductivity
  - decomposition
  - thermal contact

Instrument
- Instrumental effects:
  - crucible
  - signal-time constant
  - baseline stability
  - stabilization time
  - calibration

To gain a better understanding of the effect of these different factors, a number of measurements will now be presented and discussed. All the measurements were performed with a DSC822$^e$ equipped with an automatic sample robot. The instrument was calibrated with indium and zinc.

## Application examples

### Melting of metals

In general, the melting point of pure substances is determined as the onset temperature of the peak. For physical reasons, the side of the melting peak before melting is a straight line. The enthalpy of fusion is determined from the peak area. As a result of the given thermal conductivity, melting takes place over a certain period of time. The peaks are therefore much broader at higher heating rates.

With the DSC822$^e$, the melting point of indium can be determined over a wide range of heating rates (Fig. 1). Due to the integrated FlexCal® calibration system, onset temperatures and the enthalpies of fusion are independent of the heating rate. This ensures that the DSC measures reliably at high heating rates and that accurate temperature and heat flow values are obtained.

To improve heat transfer, it is advisable to perform fast measurements in light crucibles. The measurements used for the evaluation in Figure 1 were done in 20-µl aluminum crucibles.

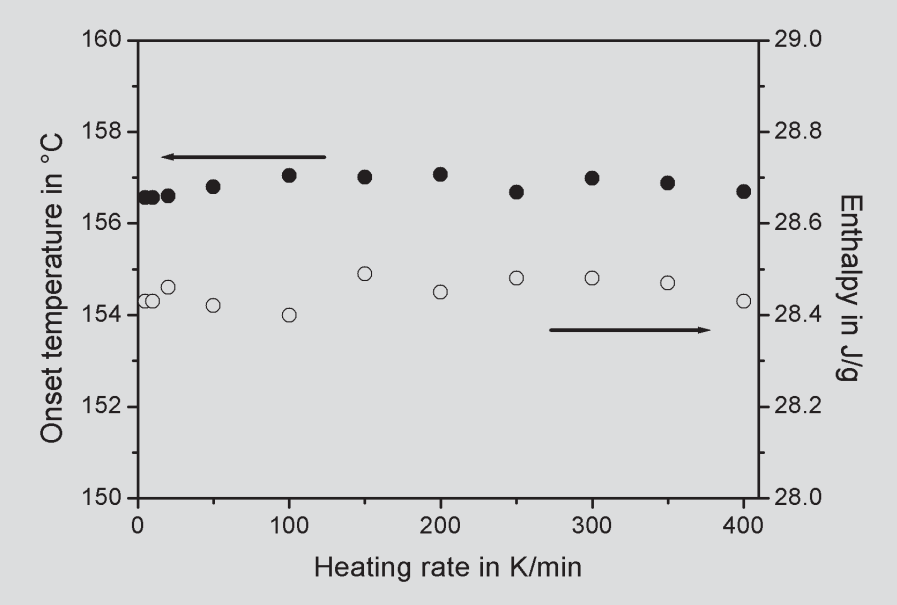


Fig. 1. Onset temperatures and enthalpies of the melting peak of indium at different heating rates.

In summary, one can say that
- onset temperatures can be determined accurately
- the same calibration procedures as with conventional DSC (heating rate to 20 K/min) can be used.

### Curing of resins

Reaction temperatures should also increase with increasing heating rates. To follow the complete reaction, one must measure to higher final temperatures. At high heating rates, the reaction peak is possibly shifted to such high temperatures that the sample begins to decompose. The occurrence of a decomposition reaction can be verified through measurement of the glass transition temperature after the reaction.

The example in Figure 2 shows the results of a curing reaction using a reactive coating powder (KU600) as an example. Heating rates of up to 200 K/min were used. As expected, the glass transition temperature is shifted to higher temperatures at higher heating rates. It can also be seen that the chemical reaction is shifted to higher temperature. The temperature of the peak maximum of the reaction shows a linear relationship with the logarithm of the heating rate. The increase is determined by the activation energy. As shown in Figure 3, the measurement result corresponds to the predicted behavior. The reaction enthalpy is practically independent of the heating rate.
The sample has a built-in «temperature calibration system» – the accelerator, which melts at 208 °C. As expected, this melting process is independent of the heating rate and proves that the shifts of the other characteristic temperatures are not artifacts. The results are summarized in Table 1.

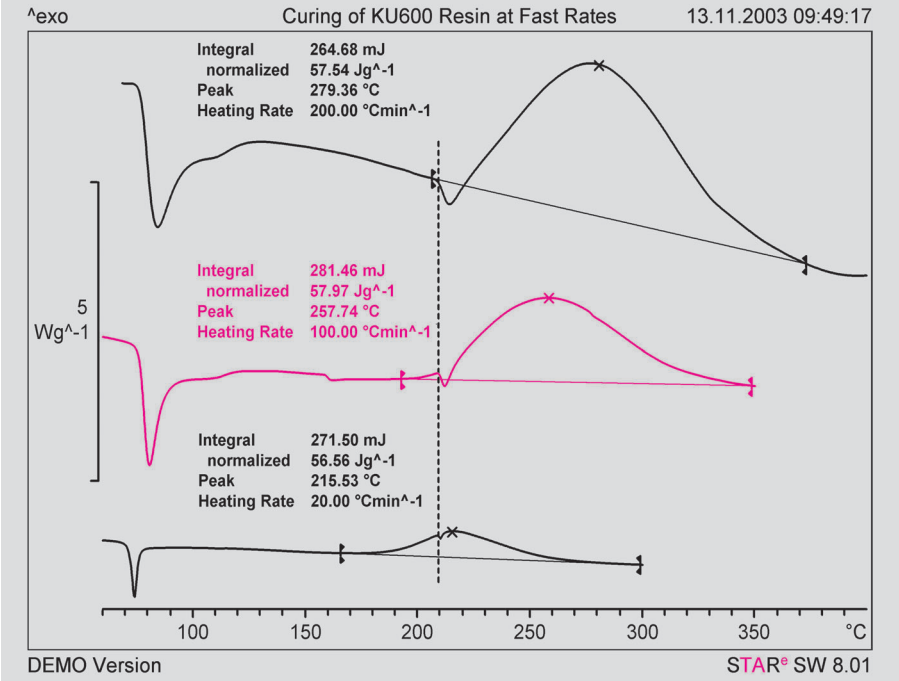


Fig. 2. Curing of KU600 powder at high heating rates.

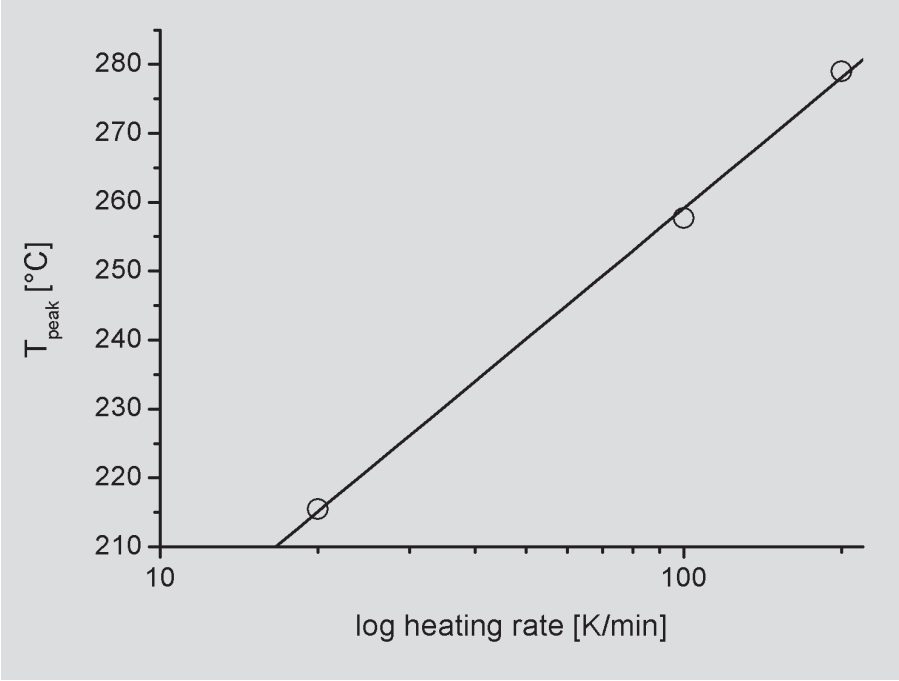


Fig. 3. Peak temperature of the curing reaction of KU600 as function of the logarithmic heating rate.

| Heating rate [K/min] | $T_g$ onset [°C] | $T_{peak}$ reaction [°C] | $T_f$ accelerator [°C] | $\Delta H_r$ [J/g] |
|---|---|---|---|---|
| 20 | 71.2 | 215.5 | 207.3 | 56.56 |
| 100 | 75.4 | 257.7 | 208.3 | 57.97 |
| 200 | 75.7 | 279.4 | 208.7 | 57.54 |

Table 1. Characteristic thermoanalytical data of the curing reaction of KU600.

## Melting of PET

Amorphous polyethylene terephthalate (PET) exhibits cold crystallization and the heating rate determines how much crystalline material is formed and hence the degree of melting that takes place. Figure 4 displays several curves of PET normalized in heat capacity units measured at heating rates between 10 and 300 K/min. After the glass transition at about 80 °C, cold crystallization occurs. The PET used for these measurements melts at 240 °C. With increasing heating rates, cold crystallization shifts to higher temperatures due to the kinetic processes involved in nucleation. The smaller peak areas indicate that with increasing heating rates the degree of crystallinity decreases. The curves measured at lower heating rates do not characterize the original material because the main effects (crystallization and melting) originate during the actual measurement itself. The curve measured at 200 K/min shows only weakly induced processes and a very small melting peak. The absence of the melting peak at 240 °C on the curve measured at 300 K/min shows that in this case no cold crystallization at all has occurred. This curve characterizes the original material. At first sight only the glass transition is visible. A closer examination of the curve revealed a very small endothermic peak at about 150 °C (marked with an arrow in Fig. 4).

This peak, which occurs between 140 and 160 °C, is shown on an expanded ordinate scale in Figure 5. At lower heating rates the peak is masked by cold crystallization. The effect responsible for this peak is the melting of a small amount of crystals that were formed during cooling in manufacture. The peak characterizes the original crystallinity of the material (about 1%). The low melting temperature indicates the imperfect structure of the crystallites.
The experimental results show that at a high heating rate of 300 K/min, the original state of the material can be characterized because no cold crystallization occurs during the experiment.

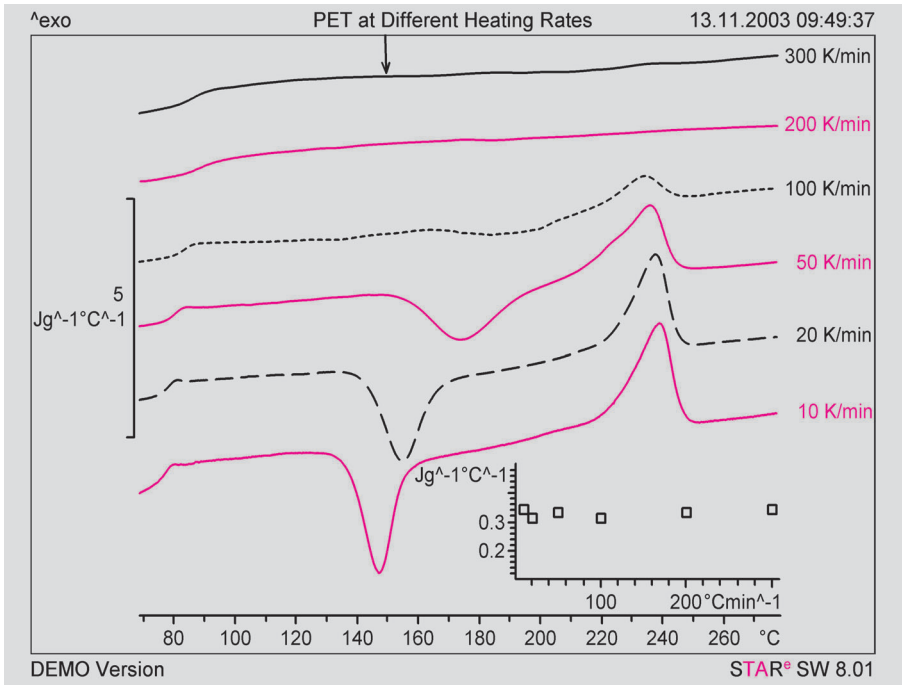


Fig. 4. DSC curves of amorphous PET, normalized to initial sample weight and the heating rate (specific heat capacity). Sample weight was less than 1 mg. Data sampling interval was 0.1 seconds.

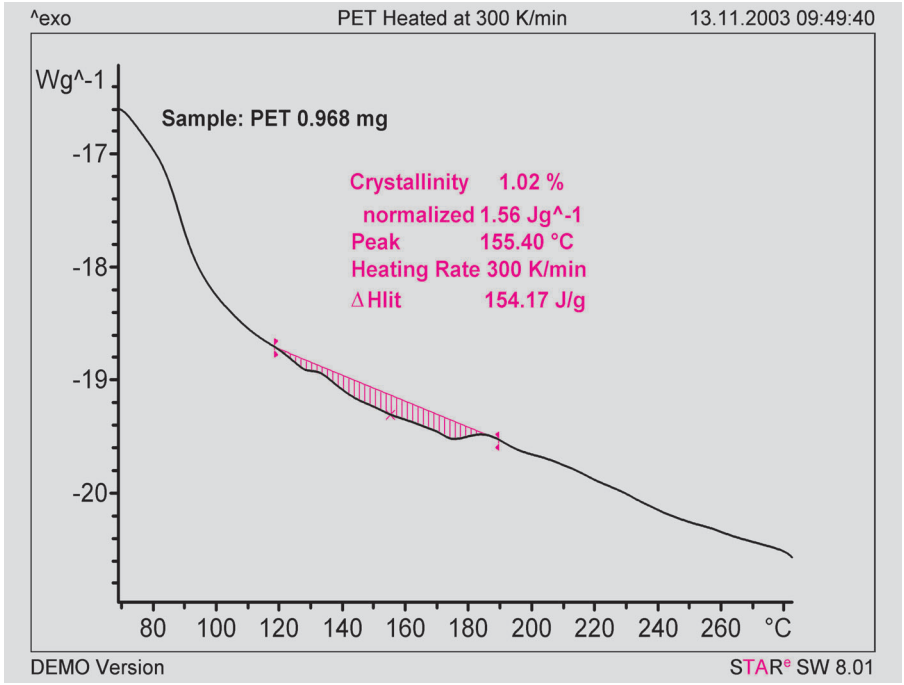


Fig. 5. Melting peak of small crystals formed in amorphous PET during cooling in production.

The diagram inserted in Figure 4 displays the step height of the glass transition at different heating rates.

As expected, $\Delta c_p$ is independent of the heating rate. This result shows that it is possible to achieve correct quantitative results even at high heating rates.

### Liquid crystal transitions

Azoxydianisole melts at 118 °C and then exhibits a liquid crystal transition at 135 °C. Both effects are independent of the heating rate. This substance can also be measured at very high heating rates as shown in Figure 6. At 200 K/min the melting peak is broadened due to the finite heat transfer in the sample. The small liquid crystal transition can still however clearly be seen as a shoulder.
The inserted diagram shows that the two effects can however be clearly separated using a deconvolution routine.

### Polymorphic transitions

The phase behavior of organic substances can also be investigated at high heating rates. This is shown using phenylbutazone as an example. In the crystalline form this substance melts at 106 °C. If the melt is shock-cooled, amorphous material is produced. On heating, the glass transition occurs at -5 °C followed by cold crystallization and then melting of two polymorphic phases. This behavior is shown in Figure 7 using heating rates of 50, 100 and 150 K/min.
It can be seen that, at higher heating rates, the crystallization peak is shifted to higher temperatures due to kinetic reasons. The decrease of the enthalpy of crystallization with increasing heating rate shows that less material is able to crystallize. Due to the high heating rate, the time for crystal growth between the beginning of cold crystallization and melting is very short.
The polymorphic phases formed melt at 98 and 106 °C. The transition temperatures of both polymorphic phases are independent of the heating rate. The areas of the melting peak and crystallization peak correspond to one another.

## Summary

The following table summarizes the advantages of using high heating rates:

| Advantages |
|---|
| Suppression of kinetically controlled effects (e.g. cold crystallization → measurement of the original crystallinity). |
| Simulation of production conditions. |
| Signal amplification due to the more rapid heating rate for<br>- small samples<br>- for samples that exhibit only weak transitions. |
| High heating rates appreciably shorten the measurement time. |

As with many other techniques, the advantages are offset by certain limitations in other respects.
Possible limitations that should be considered are:

| Limitations |
|---|
| High heating rates degrade temperature resolution (e.g. separation of peaks becomes poorer or even impossible). |
| There are no standards (up until now) for the application of high heating rates. |
| Small samples are not representative of the sample as a whole.<br>Sample preparation demands special care. |
| Higher heating rates necessitate higher end temperatures in methods because the peaks become broader. At higher end temperatures the risk of sample decomposition is greater. |
| Higher heating rates necessitate a higher measurement signal data sampling rate. |

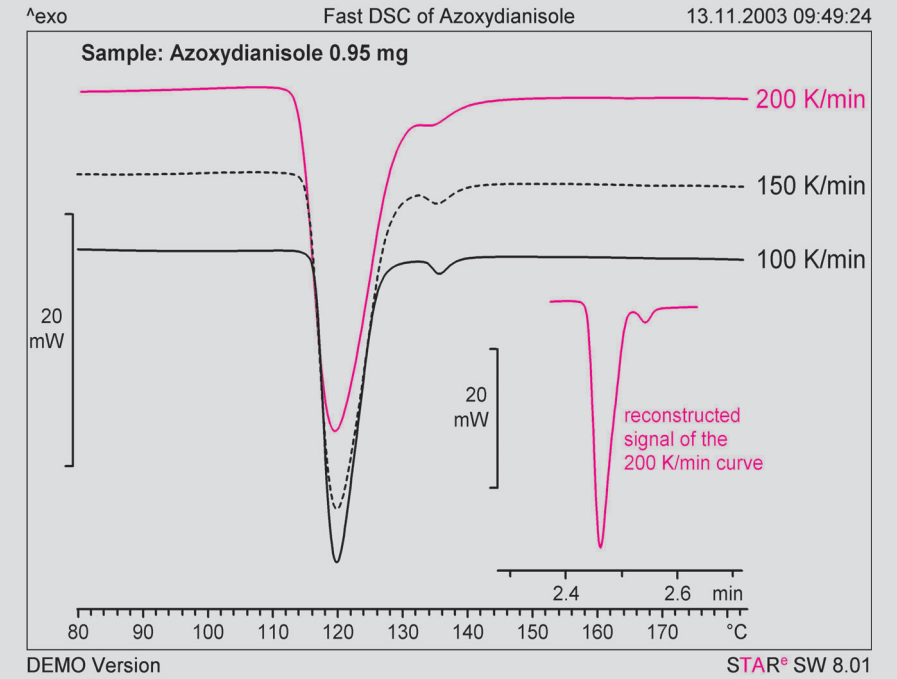


Fig. 6. Melting peaks of azoxydianisole measured at different heating rates.

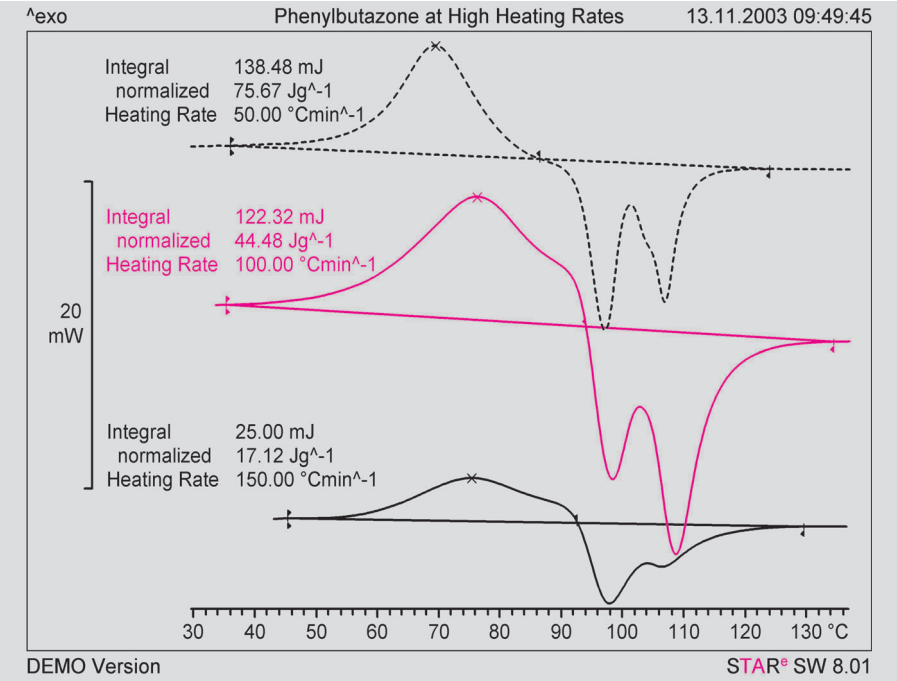


Fig. 7. Phenylbutazone measured at different heating rates.

## Conclusions

The DSC822$^e$ can measure samples at very high heating rates. FlexCal® technology ensures that the measured temperatures remain independent of the heating rate. The short response time of the DSC sensor results in rapid stabilization of the signal so that starting temperatures do not have to be very low.
The influence of the heating rate on the effect to be investigated should always be carefully considered beforehand. In general, higher heating rates lead to larger thermal gradients in the sample. This can influence the kinetics of processes, e.g. nucleation in connection with crystallization is significantly affected.
Furthermore, peaks are broadened due to smearing. To reduce these effects, it is best to use light crucibles and optimize the thermal contact between the sample and the crucible. Small, thin samples reduce the formation of temperature gradients within the sample. The use of commercially available crucibles allows an automatic sample changer to be used.

Higher heating rates permit kinetic processes to be studied over a large dynamic range. Undesired processes that occur during the measurement (e.g. cold crystallization) can be suppressed so that the measurement curve characterizes the original material.

# New in our sales program

## TMA/SDTA841$^e$

We are once again pleased to introduce a new instrument.
The TMA/SDTA841$^e$ complements the TMA/SDTA840 and extends the previous temperature range available in thermomechanical analysis (TMA). The new measuring module allows you to analyze polymeric and other materials in the range -150 °C to 600 °C.

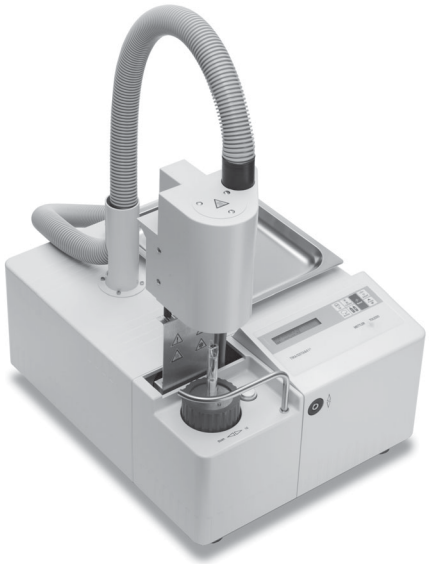

Fig. 1. The new TMA/SDTA841$^e$ module.

Thermomechanical analysis measures the dimensional changes of a sample as a function of temperature. The characteristic values and properties most frequently studied are:

- expansion coefficients
- glass transition temperatures
- softening temperatures
- solid-solid transitions
- melting behavior
- swelling behavior and
- elastic behavior.

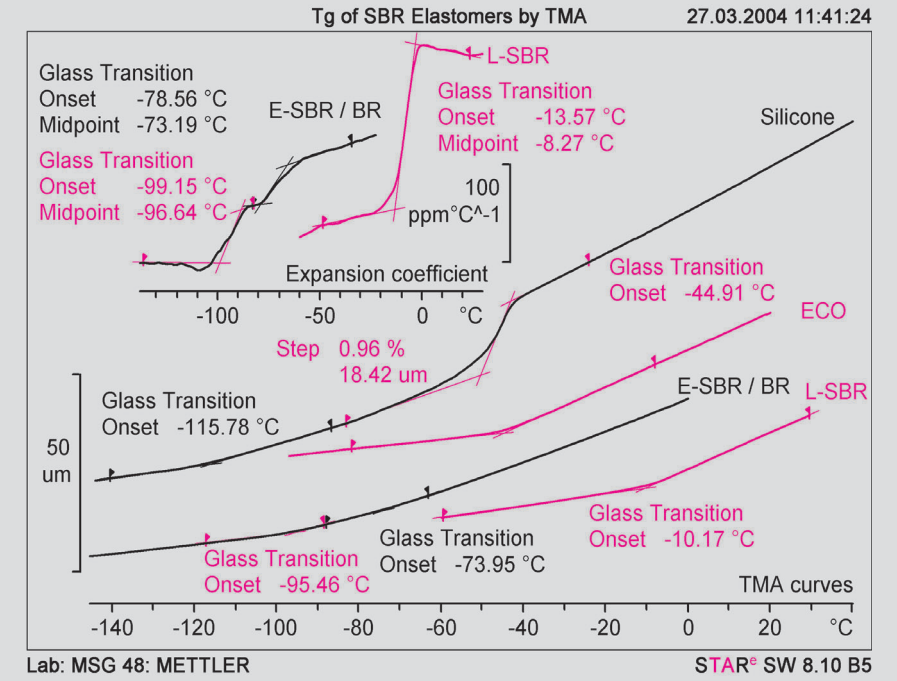


Fig. 2. TMA is an excellent method for determining glass transitions and expansion coefficients. The figure shows the expansion behavior of two rubber samples (E-SBR: emulsion SBR; L-SBR: solution SBR). Glass transitions are often difficult to see on TMA curves. They are however immediately apparent as a step change on the expansion coefficient curve.

### Typical areas of application

| Industry | Applications |
|---|---|
| Plastics (elastomers, thermosets, thermoplastics) | Coefficient of thermal expansion, glass transition, creep behavior |
| Electronics industry | Glass transition, coefficient of thermal expansion, delamination |
| Paint/lacquers/adhesives/coatings | Softening point |
| Textile fibers | Expansion and shrinkage behavior |
| Packaging (films) | Expansion and shrinkage behavior |
| Chemical (organic and inorganic materials, metals, pharmaceutical products) | Coefficient of thermal expansion and expansion behavior, solid-solid transitions |
| Universities | Dimensional changes under the most varied conditions |

### SDTA signal

The sample temperature is measured very close to the sample by means of a sheathed K-type thermocouple.
A thin quartz glass coating protects it against direct contact and contamination. This means that temperature adjustment can be performed using the melting points of pure metals and/or the length change of suitable standards.

Fig. 3. Quartz glass sample support with the K-type thermocouple for sample temperature measurement.

The SDTA signal is the difference between the reference temperature calculated with a model and the measured sample temperature (US Patent 6146013).
This means that, besides the length change, the simultaneously measured DTA signal (SDTA) is also available as a measurement quantity. This can often be of great help when interpreting a measurement curve.

### Gastight measuring cell

The measuring cell can be purged with gas in order to measure samples under defined atmospheric conditions just as in the TMA/SDTA840.

### Automation

The furnace opens and closes at the stroke of a key, guaranteeing easy and reliable operation.

### Cooling

The liquid nitrogen cooling system has been completely automated; manual refilling is not necessary. This simplifies operation, improves reproducibility and allows measurements to be performed over a long period of time.

### Thermostating

The mechanical part of the measuring cell is incorporated in a thermostated housing. This minimizes drift and guarantees excellent accuracy for the determination of expansion coefficients.

### Deformation modes

Different accessories enable you to perform measurements on solid samples, foams, films and fibers.

The TMA/SDTA841$^e$ supports the following measurement modes:

- Expansion
- Penetration
- Tension
- Bending
- Swelling

The DLTMA mode (dynamic load TMA) allows you to study the elastic behavior of materials.
In DLTMA the force exerted on the probe alternates automatically between two values.

### Overview of the TMA/SDTA841$^e$ specifications

| | |
|---|---|
| Wide measurement range | +/- 5.0 mm |
| High resolution | 0.6 nm (over the whole measurement range) |
| Long sample lengths | up to 20 mm |
| Large force range | -0.1 to 1 N |
| High force resolution | 0.13 mN |
| Wide temperature range | -150 °C to 600 °C |
| Cooling system | automatic liquid nitrogen cooling |
| High temperature accuracy | +/- 0.35 K |
| SDTA resolution | 0.005 K |
| Automation | automatic opening of the furnace with keystroke |
| DLTMA mode | ≤ 1 Hz |
| Options | gas controller<br>switched line socket |

# UV-DSC

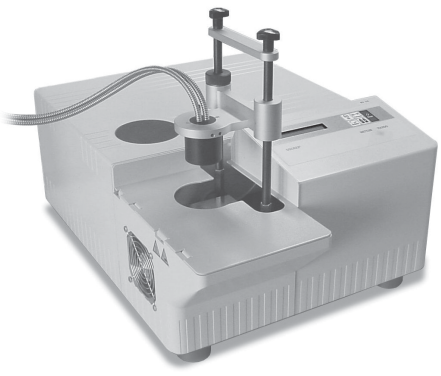

Fig.1. DSC822$^e$ with the UV-DSC accessory.

The DSC module is easily converted to a UV-DSC system by means of a special accessory.

The UV-DSC system allows you to study the influence of temperature, UV light intensity and exposure time on curing processes. The sample is held isothermally at a particular temperature and exposed to UV light for a defined period of time. The reaction of the sample to the light is measured with the DSC.

Light curing systems are used

- to shorten processing times and/or
- to avoid exposing sensitive materials to high temperatures.

Nowadays, light curing systems are used for all kinds of coating applications (e.g. in the automobile industry) and in dentistry (curing fillings).

The UV-DSC accessory can be easily installed or removed by the user.

# Kinetic studies of complex reactions
# Part 2: Description of diffusion control

*Dr. Jürgen Schawe*

## Introduction

Cross-linking reactions of «hot curing systems» are complex reactions. Depending on the reaction conditions, an initially chemically controlled reaction can change and become diffusion controlled. The reaction rate thereby decreases rapidly. The reaction almost stops. The reason for this is chemically induced vitrification as a result of which the material changes from a liquid to a glassy state.
In the first part of this study [1], the curing reaction of the a two-component epoxy resin consisting of the diglycidylether of bisphenol A (DGEBA) and diaminodiphenylmethane (DDM) as hardener or curing agent was investigated by DSC and evaluated using the Model Free Kinetics (MFK) software. Here it was shown that curing at heating rates greater than 1 K/min is chemically controlled over the entire reaction range.

By means of MFK, it is possible to correctly predict the course of an isothermal reaction right up to vitrification. If the glass transition temperature is known as a function of conversion, MFK can be used to estimate the time at which the material vitrifies in an isothermal reaction.
MFK must be extended in order to describe the complete course of a curing reaction that includes the transition from chemically to diffusion-controlled kinetics [2-4]. In this article, MFK is enhanced sufficiently for it to take the effect of diffusion control on the reaction kinetics into account.

## Prediction of chemical behavior

### The conversion curve

If MFK is applied to DSC curves that were measured at sufficiently high heating rates, one obtains activation energy curves as a function of conversion that describe a purely chemically controlled reaction (curve a in Fig. 2 of Part 1 [1]). The activation energy curve can then be used to calculate the isothermal course of the reaction. A comparison of the conversion curve calculated using MFK and the measured conversion curve for $T_{react}$ = 100 °C is displayed in Figure 1.

Up until about 40 min, the measured curve agrees well with the MFK prediction. In this range the cross-linking reaction is chemically controlled. Afterward, the influence of diffusion control increases and the measured reaction proceeds more slowly.
A comparison of the two curves allows the influence of diffusion control on the reaction kinetics to be estimated.
The reaction rate is described by the equation

$$\frac{d\alpha}{dt} = \left[\frac{d\alpha}{dt}\right]_{chem} f_d(\alpha) \qquad (1)$$

where $d\alpha/dt$ is the reaction rate (derivative with respect to time of the measured conversion curve), $[d\alpha/dt]_{chem}$ is the reaction rate of the chemically controlled reaction (obtained using MFK) and $f_d(\alpha)$ is the diffusion control function that describes the influence of diffusion control on the reaction kinetics. $f_d$ can be determined according to eq (1) by division of the measured reaction rate and the reaction rate calculated by MFK (see Fig. 1).

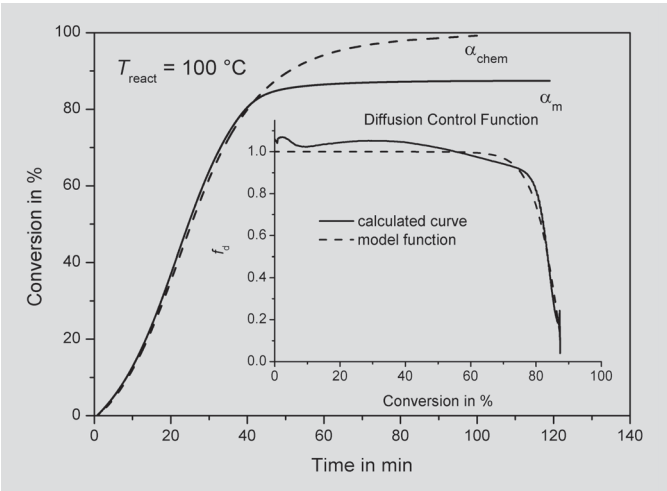


Fig. 1. Conversion as a function of time at a reaction temperature of 100 °C. $\alpha_m$ is the measured curve and $\alpha_{chem}$ is the prediction with MFK using the activation energy curve (a) in Figure 2 from Part 1 [1].
The inserted diagram displays the diffusion control function, $f_d$. The continuous curve is calculated from the conversion curves according to eq (1). The dashed line corresponds to the model function from eq (2).

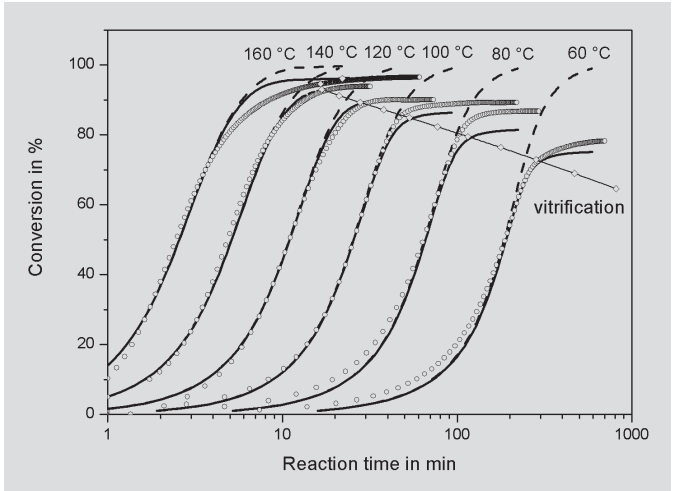


Fig. 2. Conversion as a function of reaction time for isothermal reactions at different temperatures. Dashed line: result from MFK ($\alpha_{chem}$); continuous line: result of the calculation according to eq (4), circles: measured curves. The line with the squares marks the vitrification. These values were taken from Figure 4.

Since the diffusion control is connected with the vitrification, a model function is introduced for $f_d$ that takes into account the conversion-dependence of the glass transition temperature [4]:

$$f_d(\alpha, T_{react}) = 1 - \left(1 + \frac{1}{2}\left(\frac{T_{react} + \Delta T - T_g(\alpha)}{\Delta T}\right)^3\right)^{-1} \quad (2)$$

The only parameter in this equation is $\Delta T$. This parameter describes the width of the glass transition. $\Delta T$ is set to 20 K, the width of the glass transition of the fully cured material.
A modified DiBenedetto equation [5] is used to describe the glass transition temperature as a function of conversion:

$$T_g(\alpha) = \frac{\lambda\,\alpha(T_{g1} - T_{g0})}{1-(1-\lambda)\alpha} + T_{g0} \quad (3)$$

where $T_{g0}$ and $T_{g1}$ are the glass transition temperatures of the unreacted and fully reacted sample. $\lambda$ is a fit parameter. The parameters $\lambda = 0.31$ and $T_{g1} = 169.3$ °C were determined [1] by means of curve fitting to the measurement results from postcuring experiments [1]. $T_{g0} = -18.3$ °C was measured by DSC at 10 K/min [1].
As can be seen in Figure 1, the model function calculated according to eq (2) agrees very well with the experimentally determined diffusion control function. Using eqs (1) and (2), a complete prediction of the kinetics of such complex reactions can be made based on MFK.

The isothermal conversion curves were calculated using a spreadsheet. The change of conversion at a reaction step $\Delta\alpha_i$ is given by

$$\Delta\alpha_i = (\alpha_{chem,i} - \alpha_{chem,i-1}) f_d(\alpha_{i-1} + \Delta\alpha_i) \quad (4)$$

where $\alpha_i$ is the sum of all the previous reaction steps:

$$\alpha_i = \sum_{j=1}^{i} \Delta\alpha_j \quad (5)$$

$\alpha_{chem,i}$ are the individual values of the MFK prediction for the isothermal reaction at $T_{react}$.
At the beginning: $\Delta\alpha_0 = \alpha(t_{react} = 0) = 0$ and $\Delta\alpha_1 = \alpha_1 = \alpha_{chem,1}$.
The indices i and j (i,j = 0,1,2,3...) describe the number of the base points.

The conversion calculated according to eq (4), the results of the MFK prediction and the measurements are displayed in Figure 2 and show agreement of the measurements with the predictions of MFK before vitrification begins. The results of the calculation taking into account the diffusion control function describe the entire reaction.

## Maximum conversion

After vitrification, the reaction becomes more and more diffusion controlled and then practically stops at a maximum conversion, $\alpha_{max}$, which is smaller at lower reaction temperatures. $\alpha_{max}$ is an important technological quantity because it indicates the conversion up to which the material can react. A greater conversion can only be reached by raising the reaction temperature.
The calculated values of $\alpha_{max}$ originate from the end points of the calculations according to eq (4) (Fig. 2). Figure 3 shows that they agree with the measured values within the limits of measurement uncertainty.

## The vitrification time

Another important factor for describing curing reactions is the vitrification time, $t_v$. This is important from the technological point of view because it indicates the time after which the resin is no longer liquid. At the vitrification time, $T_g = T_{react}$. The conversion-dependence of $T_g$ is used to calculate $\alpha$ at $t_v$ (eq (4) and Fig. 4 in [1]). The time for the conversion curve to reach this value is called the vitrification time. $t_v$ was determined from the two conversion curves, one value calculated by MFK [1] and the other according to eq (4) taking the diffusion control function into account. The values are displayed together with the experimental results from postcuring measurements (Fig. 3 in Part 1 [1]) in Figure 4. It can be seen that the vitrification time can be predicted with very good accuracy on the basis of both calculations. Only at high reaction temperatures (greater than 130 °C) is the time calculated by MFK somewhat too short. If the diffusion

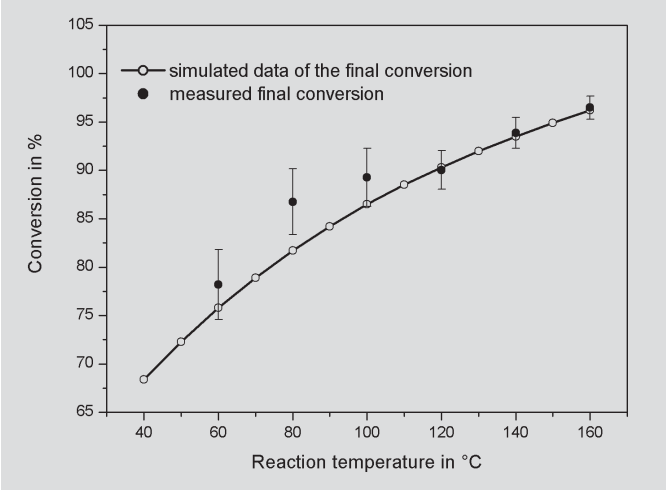


Fig. 3. The maximum conversion for an isothermal reaction as a function of the reaction temperature.

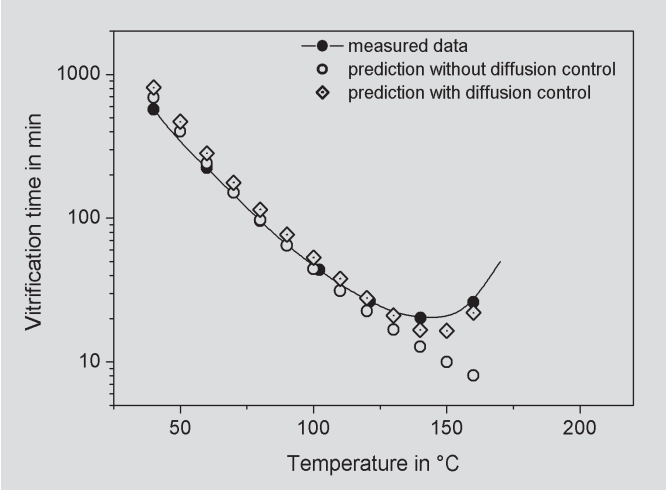


Fig. 4. Vitrification time as a function of reaction temperature for an isothermal reaction. The measured data (filled circles) were determined from postcuring measurements (Fig. 3 in Part 1 [1]). The empty circles show the MFK results and the squares have been calculated taking the diffusion control function into account.

control function is taken into account, $t_v$ is correctly predicted over the entire temperature range. MFK alone without taking diffusion control into account is adequate to predict the storage life.

## Conclusions

MFK adequately describes the reaction kinetics if the DSC measurements are made at sufficiently high heating rates so that the reaction remains chemically controlled. If the material vitrifies during the reaction, the kinetics changes from being chemically controlled to diffusion controlled. In this case, a better description of the kinetics can be achieved through the introduction of a diffusion-control function. This function enhances MFK in such a way that it also describes the transition to diffusion control. It is then possible to calculate the maximum conversion that can be reached.

To predict the kinetics of the curing reaction with MFK requires at least three dynamic DSC measurements performed at different heating rates. Furthermore, at least four (better six) postcuring measurements to determine the conversion dependence of the glass transition temperature are needed. The glass transition temperature of a fully cured sample should be determined in an additional experiment. In comparison to the time required for isothermal measurements, the use of MFK presents a considerable saving of time.

## Literature


[1] *J. Schawe, UserCom 18 (2003) 13.*
[2] *S. Vyazovkin, New J. Chem., 24 (2000) 913.*
[3] *S. Vyazovkin N. and Sbirrazzuoli, Macromol. Rapid Commun, 21 (2000) 85.*
[4] *J.E.K. Schawe, J. Thermal. Anal. Cal., 64 (2001) 599.*
[5] *J.P. Pascault and R.J.J. Williams, J. Polym. Sci.: Part B: Polym. Phys. 28 (1990) 85.*


Previous UserCom articles can be downloaded via
http://www.mt.com/home/products/en/lab/thermal/analysis/141401.asp

# Curing kinetics of phenol-formaldehyde resins


*Felisa Chan, Guangbo He, Yves Bedard and Bernard Riedl, Université Laval, Dept of Wood Science and CERSIM, Ste-Foy, Qc, Canada, G1K 7P4*


## Introduction

DSC and TGA are well-known techniques commonly used to perform kinetic studies of materials in thermal analysis (TA). Knowledge of the influence of temperature on the reaction rate of phenol-formaldehyde resins (PF resols) allows the polymerization rate to be predicted. This is of great practical importance for example in the manufacture of wood composite materials or for the storage of the resins.

Most of the resol cure kinetics reported in the literature have been obtained using the Borchardt-Daniels method. Here only one run at one heating rate (dynamic measurement) is necessary to obtain the desired kinetic parameters. The kinetic parameters are, however, usually heating rate dependent and care must be taken when evaluating and interpreting the results. Likewise, the activation energy is often assumed to be constant throughout the reaction. This is, however, not true for complex curing reactions such as occur in phenolic resins. A phenol-formaldehyde (PF) resin may be of low viscosity at the start of the run and fit the assumptions for dilute solutions. But as the curing reaction proceeds, the material undergoes gelation, i.e. changes from a liquid to a rubbery state, and possibly vitrifies (transition from a rubbery to a glassy state). The cross-linking reduces molecular mobility and results in the process changing from being kinetically controlled to diffusion-controlled [1].

The model-free kinetics (MFK) method, developed by Vyazovkin [3-5] is based on the assumption that the activation energy, $E_a$, is dependent on the conversion ($\alpha$). At a particular conversion, the activation energy, $E_a$, is independent of the heating rate. Evaluation by MFK requires at least three dynamic measurements performed at different heating rates.
Since the reaction of phenol and formaldehyde under alkaline conditions to a PF resin is complex, MFK evaluation seems a suitable method to describe the curing behavior.

## Experimental details

A liquid PF resol consisting of low and high molecular weight fractions (1:1 by weight) was synthesized in the laboratory.

The high molecular weight fractions were prepared with a formaldehyde-to-phenol ratio of 2.2 and a ratio of NaOH to phenol of 0.35; the low molecular weight fractions had ratios of 2.2 and 0.17. The resulting resin had a solid content of 46% («pan method»).

A METTLER TOLEDO DSC 20 with STARe software was used for all the thermoanalytical measurements. Since such adhesive formulations contain water, re-usable 30-µl high-pressure steel crucibles capable of withstanding vapor pressures up to 10 Mpa were used. The dynamic DSC measurements were performed at heating rates of 5, 10 and 20 K/min in the temperature range 25 to 250 °C. The DSC curves were evaluated with different kinetic methods (STARe software options).

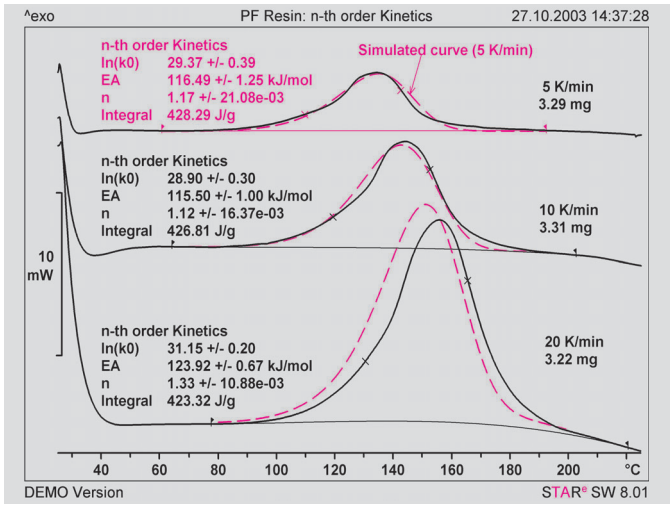


Fig. 1. DSC curves of the PF resol measured in high-pressure crucibles at 5, 10 and 20 K/min. The parameters of the $n^{th}$ order kinetics are entered for each curve. The simulated curves (red dashed lines) were calculated with the kinetic parameters from the measurement at 5 K/min.

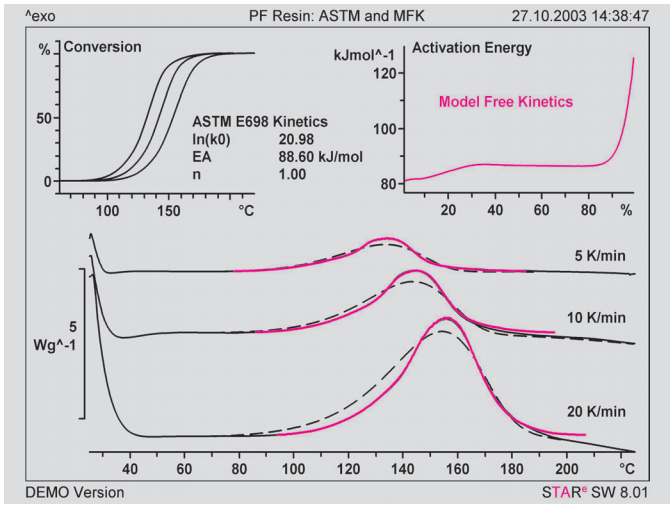


Fig. 2. Model free kinetics: Above left: the conversion curves calculated from the DSC curves (see Fig. 1) for heating rates of 5, 10 and 20 K/min. Above right: the activation energy, $E_a$, as a function of reaction conversion. The result block shows $E_a$ and $\ln(k_0)$ evaluated according to ASTM E698. Bottom half: the simulated DSC curves plotted together with the measured DSC curves. The dashed curves show the curves predicted from the ASTM parameters; the continuous red curves show the curves from MFK.

## Measurements and results

### Evaluation according to Borchardt-Daniels

Figure 1 shows the DSC curves of the PF resol measured at heating rates of 5, 10 and 20 K/min. The exothermic reaction peaks were shifted to higher temperatures at increasing heating rates due to kinetic effects. The beginning of an endothermic decomposition reaction can be seen from 200 °C onward especially in the curve measured at 20 K/min. This overlaps the end of the curing reaction. A «spline» baseline type was therefore used to integrate the DSC peaks to determine the conversion and the reaction rate. Care was taken to make sure that the total reaction enthalpy was about the same for each evaluation because it can be assumed that it is independent of the heating rate. The kinetic parameters for each measurement curve were determined using the $n^{th}$ order kinetics method according to Borchardt-Daniels (see Fig. 1 and Table 1). As the table shows, with the Borchardt-Daniels method the results change with the heating rate. $E_a$ at 20 K/min has about the same magnitude as the value published by Amen-Chen et al. [6] for liquid laboratory-synthesized PF resin ($E_a$ = 129 kJ/mol at 10 K/min).

To demonstrate how well the three values describe the curing process, the kinetic parameters were used to simulate the DSC curves. As Figure 1 shows, this was done with the parameter set for 5 K/min. The measured curve is relatively well simulated; at higher heating rates, however, the simulated curve is displaced by more than 5 K from the corresponding measurement curve. This shows that the kinetic description is only valid for the measured conditions, and that other situations cannot be accurately predicted.

Table 1 also lists the evaluation according to ASTM E698. From the three measurements, only the peak temperatures are used. The reaction order, n, is set to 1. $E_a$ and $\ln(k_0)$ differ significantly from the Borchardt-Daniels values. Differences in the kinetic parameters from multiple dynamic measurements and from isothermal measurements have also been described in [2]. The activation energy from individual dynamic measurements was more than 25% greater than that determined from multiple measurements.

| Kinetic evaluation | Heating rate | $E_a$ | n | $\ln(k_0)$ | $\Delta H_r$ |
|---|---|---|---|---|---|
| | K/min | kJ/mol | - | - | J/g |
| Borchardt-Daniels | 5 | 117 | 1.17 | 29.4 | 428.3 |
| Borchardt-Daniels | 10 | 116 | 1.12 | 28.9 | 426.8 |
| Borchardt-Daniels | 20 | 124 | 1.33 | 31.2 | 423.3 |
| ASTM E698 | | 88.6 | 1 | 21.0 | |
| MFK ($\alpha$ = 50%) | | 86.4 | | | |
| MFK ($\alpha$: 30 to 80%) | | 86.4 ± 0.3 | | | |

Table 1. Summary of the numerical results of the PF resol curing reaction.

### Evaluation with model free kinetics

Figure 2 shows the evaluation with model free kinetics. The first step is to determine the conversion curve as a function of temperature for each of the three heating rates. The same baselines as in Figure 1 were used. The diagram clearly shows that the reaction curves are shifted to higher temperatures at higher heating rates. For heating rates of 5, 10 and 20 K/min, 50% conversion was for example reached at 131.9, 141.8 and 153.3 °C. This information can already be valuable for performing the reaction process on a technical scale.

In a second step, the activation energy ($E_a$) curve is calculated as a function of conversion from the conversion curves. At the beginning of the reaction, $E_a$ increases by about 5%, and then attains a practically constant value of about 86 kJ/mol between

40 and 80%. This value is very similar to the value obtained from the ASTM E698 method. The rapid increase of $E_a$ above 90% conversion indicates a significant change in the reaction mechanism. The results of Amen-Chen et al. [6] also show a practically constant activation energy from 20% conversion onward.
The results from MFK can then be used to simulate DSC curves (Fig. 2). Comparison with the measured curves shows excellent agreement. There are small deviations toward the end of the reaction where the DSC curves are deformed through overlapping effects (decomposition).

For comparison Figure 2 also shows the DSC curves calculated using the kinetic parameters obtained from ASTM E698. Comparison with the measured curves shows that in spite of good agreement of the $E_a$ values from ASTM and MFK evaluation, the curve simulated with the ASTM parameters is significantly poorer than the curve simulated with the results obtained from MFK.
He et al. [1] report a value of $E_a$ = 60 kJ/mol (MFK method) for the PF resol described in their publication. Borchardt-Daniels evaluations tend to give higher activation energies compared with MFK and ASTM698 values. A similar observation was made by Amen-Chen et al. [6] in their pyrolysis reactions of oil-PF resins.

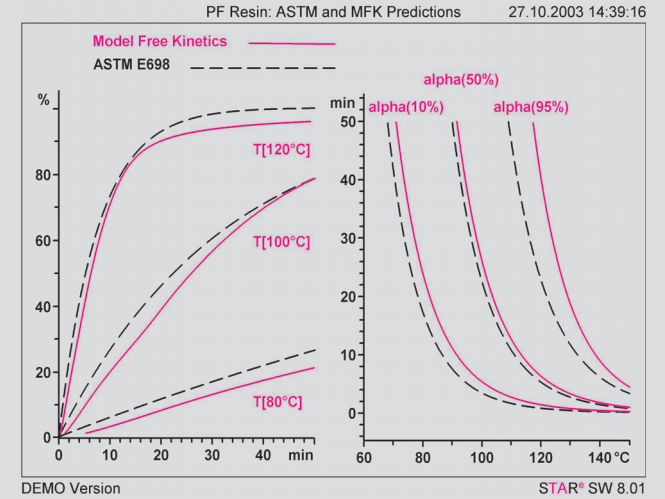


Fig. 3. Applied kinetics: prediction of conversion behavior. Left diagram: conversion as a function of time for three different reaction temperatures. Right diagram: reaction time as a function of the isothermal curing time for three different degrees of conversion. The red continuous lines show the predictions based on model free kinetics, the black dashed curves show the behavior based on the results of the ASTM E698 kinetics evaluation.

### Prediction of reaction behavior

The results of the kinetic analysis allow one to predict the course of the curing reaction under other reaction conditions. Besides the simulation of DSC curves already shown (Figs. 1 and 2), predictions of a more technical interest are summarized in Figure 3. The diagram on the left that shows conversion as a function of time answers the question, «How long does the reaction take at a particular isothermal reaction temperature?» The other diagram on the right shows how the reaction time changes with temperature for a given conversion. According to the MFK prediction, it takes for example 40 minutes to obtain a 95% degree of cure at a constant temperature of 120 °C. In contrast the prediction made on the basis of the ASTM results gives 23 min, which in view of the poor simulation of the DSC curves (Fig. 2) seems improbable.
These types of predictions are important for practical processes using PF resins, e.g. in hot press molding cycles in the manufacture of wood composite materials. Furthermore, by properly choosing the conditions, predictions can also be made with respect to the storage life of the resins.

## Conclusions

The reaction behavior of phenol-formaldehyde resins can be studied with different kinetic evaluation methods. From the results, the conversion-temperature-time behavior can be predicted and answers given to technological questions. The activation energy is often the key quantity. A comparison of the methods has shown that only model free kinetics (MFK) is able to adequately describe the complex curing reaction in most respects. The Borchardt-Daniels method can hardly determine the activation energy properly and the ASTM E698 method yields the activation energy only at the highest reaction rate (DSC peak temperature). MFK however shows the activation energy curve as a function of conversion. This can provide useful information for the interpretation of the curing mechanisms besides yielding trustworthy simulation data. It has for example been shown for PF resins in wood composites (He et. al. [1]) that the degree of cure of the resin in the wood is not so high as when the resin is used in the pure form. Diffusion of the resin in the wood, which has a porous structure, is hindered or even prevented through gelation of the adhesive.

## Literature


[1] *He, G., Riedl B., Aït-Kadi A., J. Applied Polymer Science, 87 (2003), p. 433.*
[2] *Prime, R.B., in: Thermal Characterization of Polymeric Materials. Academic Press, San Diego, (1997) p. 1636-1646.*
[3] *Vyazovkin, S., Lesnikovich, A. 165 Thermochimca Acta (1990), p. 273.*
[4] *Vyazovkin, S. Thermochimca Acta 194 (1992), p. 221.*
[5] *Vyazovkin, S., N. Sbirrazzuoli. Macromolecules (1996) 29, p. 1867.*
[6] *Amen-Chen, C., B. Riedl, C. Roy. Holzforschung. 56(3), (2002) p. 273*

# Curing of powder coatings using UV light

*Dr. Markus Schubnell*

## Introduction

Today, powder coating technology is applied to a wide range of different materials (wood, plastics, metals, etc.).

Besides the excellent properties of such coatings, their use also offers important ecological advantages. For example, unlike liquid paints, no solvents are used so that only negligible amounts of volatile organic compounds (VOCs) are released into the atmosphere.

The powder coating is usually sprayed onto the parts to be coated and then cured. The curing or cross-linking process is then performed either thermally in an oven (typically at about 180 °C) or by means of UV light. Curing with UV light has the great advantage that materials sensitive to temperature (such as wood or plastic products) can be coated.

In practice, a combined IR/UV processing line is used for the UV curing of powder coatings. In the IR zone, the powder «melts» under the influence of the infrared (IR) light and forms a homogeneous film on the substrate to be coated. The liquid film so formed is then cured in the UV zone within seconds or minutes.

This article describes how DSC can be used to investigate the UV curing behavior of powder coatings.

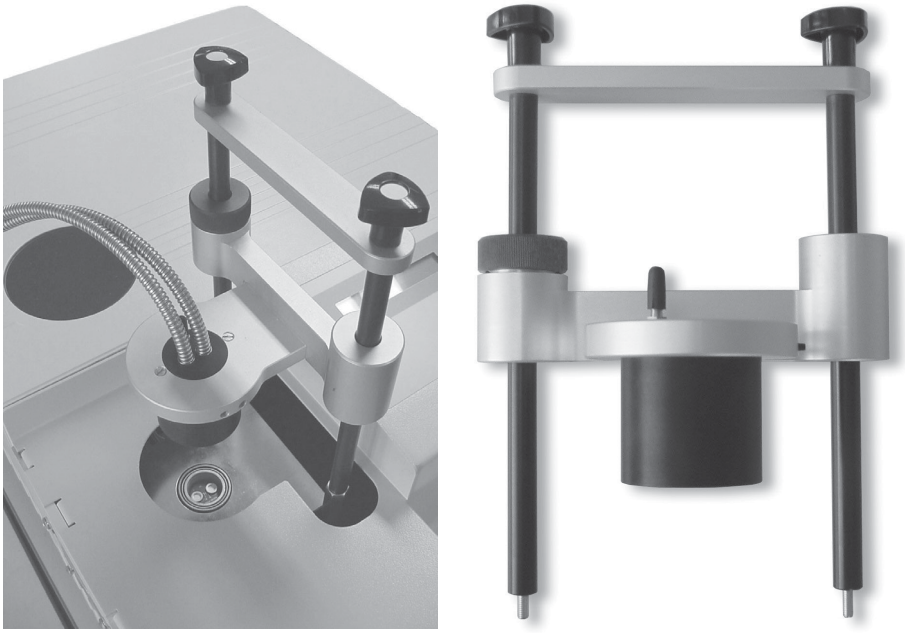

Fig. 1. Left: the UV-DSC accessory. Right: support for the quartz glass fiber bundle.

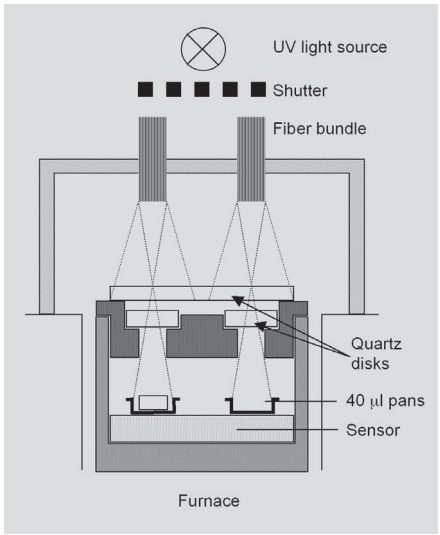


Fig. 2. Optical setup for projecting UV light into the DSC822e.

## Experimental details

### Design of the UV-DSC system

The measurements were performed with a METTLER TOLEDO DSC822e equipped with an accessory that allowed the sample to be exposed to UV light.

The UV-DSC system is pictured in Figure 1 and a schematic diagram is shown in Figure 2.

The light source used was a Hamamatsu «Lightningcure 200» system. The spectrum of the built-in mercury-xenon lamp is shown in Figure 3.

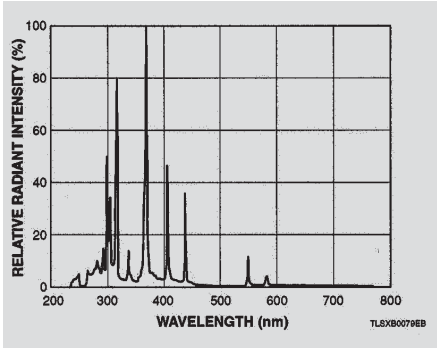


Fig. 3. Spectrum of the UV lamp used in the Hamamatsu «Lightningcure 200». The lamp emits UV light mainly in the so-called UV-A region (315-400 nm). The UV light emitted in the 290-315 nm wavelength region is referred to as UV-B light. UV light of still shorter wavelengths (down to 100 nm) is called UV-C light.

### Sample preparation and evaluation of the measurements

The sample investigated was a commercially available powder coating material used as a clear primer for wood fiberboard and chipboard surfaces. Typically 8.5 mg of the material was spread evenly over the bottom of the crucible forming a layer about 0.8 mm thick. In each case, the samples were held for 25 minutes at the temperature at which curing was to be performed. During this time interval, the sample was exposed to UV light for 15 minutes. The degree of cure was afterward

checked by measuring the glass transition temperature of the sample in a separate heating experiment at 10 K/min.
The baseline during the curing process is of course required to determine the enthalpy of cure. To a good approximation, this unknown baseline can be determined by repeating the measurement with the cured sample under exactly the same conditions (including UV exposure). Another possibility is simply to integrate the exothermic curing peak during the UV exposure interval using a horizontal baseline. Figure 4 shows that the two methods in fact yield similar results. For our experiments, only the second method was used.

## Measurements and results

With UV curing, three basic questions arise:

1. What influence do the temperature and UV light intensity have on the curing process?
2. How long does the sample have to be exposed to UV light to achieve an adequate degree of cure or cross-linking?
3. What are the optimum parameters for the cross-linking reaction?

The first two questions are investigated in more detail in the following sections. The latter point is discussed in the final conclusions.

### Influence of temperature and UV light intensity

To investigate the influence of temperature and UV light intensity on the curing reaction, isothermal DSC curves were measured at four different temperatures using three different UV light intensities.
An example is shown in Figure 5. The figure displays curves of samples that were measured at 100, 110, 120 and 130 °C while being exposed to a UV light intensity of 1.12 mW/cm$^2$ (falling on the sample). The results show that temperature does not have any appreciable influence on the enthalpy of cure at this level of light intensity. This also means that glass transition temperatures measured after curing are independent of temperature. At higher temperatures, however, the maximum heat flow increases and the peak width decreases, i.e. the curing or cross-linking reaction takes place more rapidly.

Figures 6 and 7 summarize these relationships for the different UV light intensities used. With a light intensity of 1.12 mW/cm$^2$, the width of the curing peak changes by about 20 s for a 10 K change in temperature (Fig. 6). The peak width here is defined as the full width of the peak at half the maximum peak height (**F**ull **W**idth at **H**alf **M**aximum, FWHM). The maximum heat flow (Fig. 7) changes by about 0.05 mW for a temperature change of 10 K. At a light intensity of 1.12 mW/cm$^2$, this corresponds to about 5% of the maximum heat flow. These results show that the curing temperature has an insignificant (but nevertheless clearly measurable) influence on the actual cross-linking process. In contrast, temperature has a large effect on the viscosity (and hence on flow behavior) and in turn on the uniformity of the thickness of the coating.

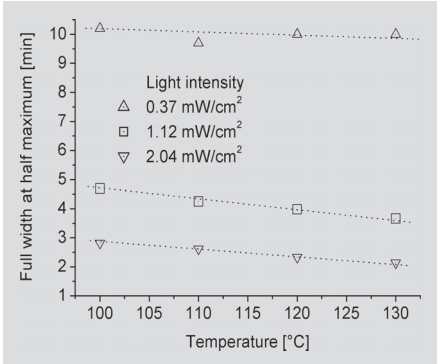


Fig. 6. Influence of temperature on the curing time for different UV light intensities. The FWHM increases by about 0.3 minutes when the temperature is reduced by 10 K.

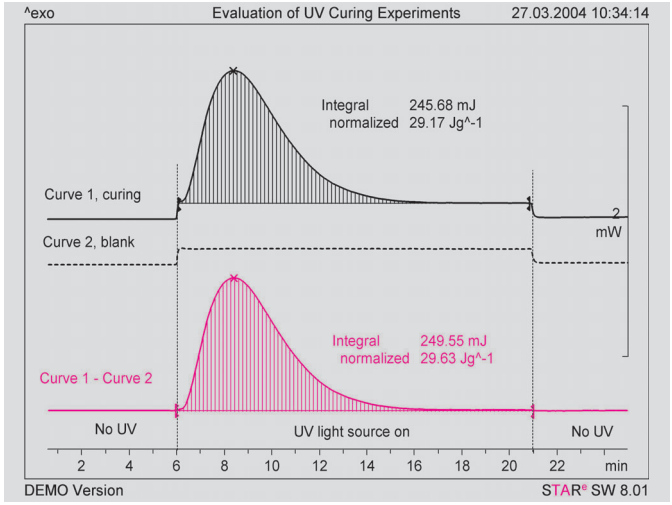


Fig. 4. Determination of the enthalpy of curing in UV-DSC experiments. The sample was held isothermally for 25 minutes at 110 °C. After 6 minutes, the shutter of the lamp was opened and the sample exposed to UV light for 15 minutes during which time the curing reaction took place. The reaction enthalpy is obtained from the measured curve (black, continuous) by integration of the exothermic curing peak. If baseline correction is not applied, a horizontal baseline is drawn at equilibrium heat flow after curing (21 minutes). Correction of the original measured curve with a baseline yields the red curve. The baseline is the black dotted DSC curve that results when the cured sample is again exposed to UV light of the same intensity for the same interval. Calculation of the reaction enthalpy, i.e. the enthalpy of cure, yields the same value with both methods within the limits of measurement accuracy.

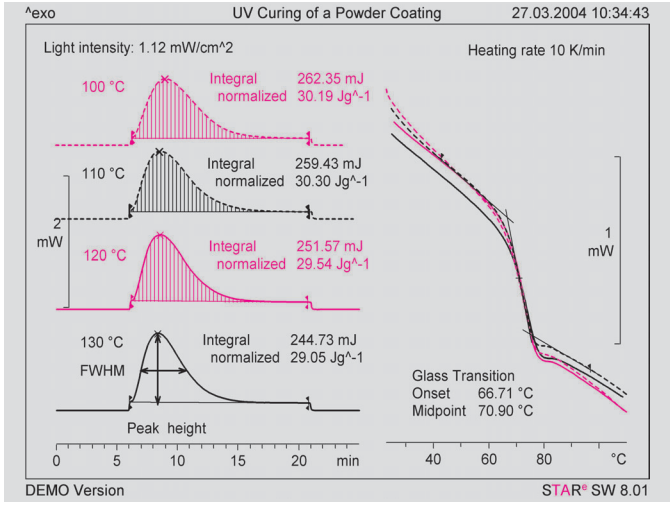


Fig. 5. Curing of a powder coating system at different temperatures using a UV light intensity of 1.12 mW/cm$^2$ (on the sample). The sample was held isothermally for 25 minutes at the given temperatures and exposed to UV light for 15 minutes. The left side of the figure displays the isothermally measured curves and the evaluation of the enthalpy of cure. The right side of the diagram shows the heating curves recorded (at 10 K/min) immediately after curing. The conclusion is that temperature has no significant influence on the degree of cure at this level of light intensity. In contrast, the widths (and therefore the heights) of the curing peaks vary with temperature (Figs. 6 and 7).

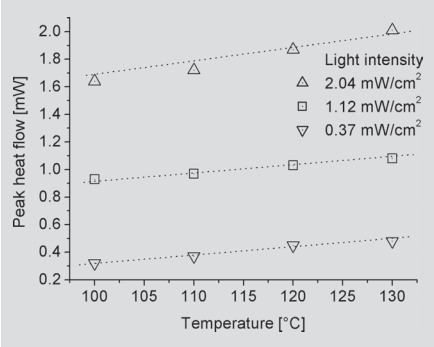


Fig. 7. Influence of temperature on the maximum heat flow during curing for different UV light intensities. The maximum heat flow increases by about 0.05 mW when the temperature is increased by 10 K.

The two figures also show that the UV light intensity strongly influences the curing time. This relationship is shown in Figure 8. If the data is approximated to a simple exponential function, the FWHM (and therefore the curing time) doubles when the light intensity is reduced by about 0.4 mW/cm².

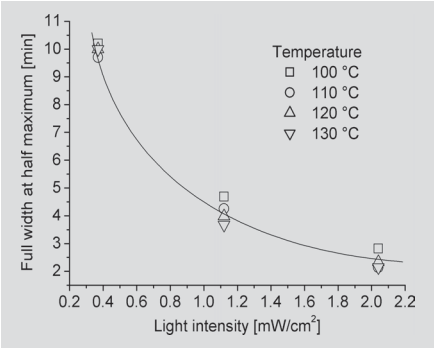


Fig. 8. Relationship between the FWHM and the UV light intensity at different temperatures. The diagram shows that the influence of temperature on the curing or cross-linking process can be neglected in the temperature and light intensity ranges used here. If an exponential relationship is assumed for the FWHM and light intensity, it shows that the FWHM approximately doubles when the light intensity is reduced by 0.4 mW/cm².

### Thermal curing (without exposure to UV light)

The powder coating system studied here can also undergo thermal curing or cross-linking. This is illustrated in the DSC measurements shown in Figure 9. The second heating run was used as baseline for the determination of the reaction enthalpy or enthalpy of cure. The measurements show that thermal cross-linking does not begin until about 180 °C. This proves that no significant degree of thermal cross-linking takes place in the temperature range in which the UV curing experiments were performed.

### Influence of the UV exposure time on the degree of cure

For a given UV light intensity, the degree of cure and hence the glass transition temperature depend mainly on the UV exposure time. Figure 10 shows the heat flow curves for the isothermal curing of samples exposed to UV light for different periods of time. The sample temperature was 110 °C and the light intensity 1.12 mW/cm². The inserted diagram in the upper right part of the figure shows heating curves of the samples measured immediately after curing (heating rate 10 K/min). From these curves, the relationship between the glass transition temperature and the degree of cure, i.e. conversion or degree of cross-linking can be plotted (Fig. 11). The degree of cure corresponds to the ratio of the reaction enthalpies of a partially cured and a fully cured sample. For practical applications, the coating should have a glass transition temperature of about 70 °C. This is achieved with a degree of cure or conversion of 80%. Figure 12 displays the conversion as a function of time for a sample that was exposed to a UV light intensity of 1.12 mW/cm² at 110 °C until it was fully cured. The diagram shows that a conversion or degree of cure of 80% is reached after an exposure time of about 5 minutes.

## Conclusions

Powder coating technology with UV light curing is used to apply high quality coatings to the surfaces of temperature sensitive materials. The influence of temperature, UV light intensity and exposure time on the curing process can easily be determined using a DSC822ᵉ equipped with a UV accessory.

The experiments clearly showed that temperature has a negligible influence on the actual curing or cross-linking process for the powder coating system studied here. Temperature does however have an important influence on the flow properties of the uncured coating material and hence on the homogeneity of the coating produced in the cross-linking reaction. A number of other studies have established that the flow behavior of this powder coating at 110 °C is optimal for the UV cross-linking process.

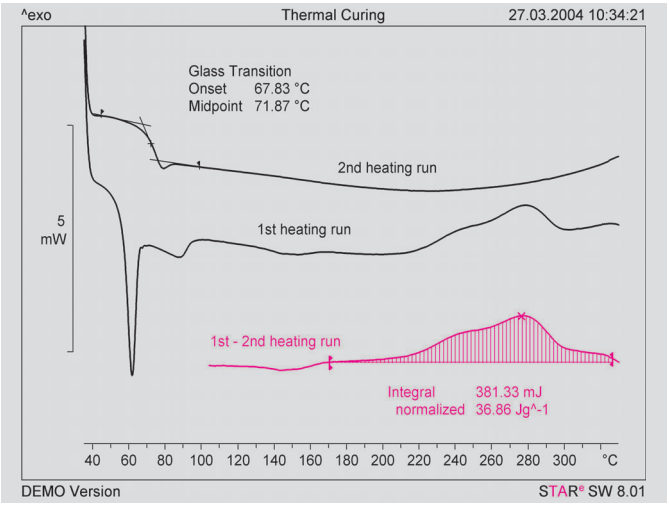


Fig. 9. Thermal curing or cross-linking reaction of a powder-coating system. The curing process begins at about 180 °C at the heating rate used here (10 K/min). Evaluation of the glass transition of the cured material yielded a midpoint value of 71.9 °C.

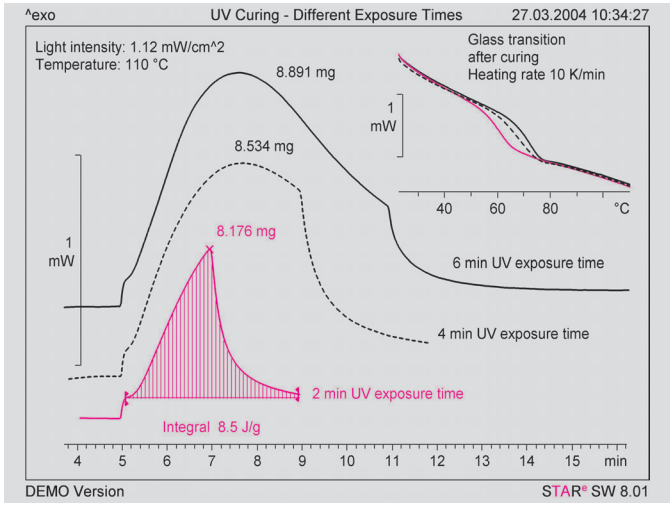


Fig. 10. Influence of UV exposure time on the degree of cure. Sample temperature 110 °C; light intensity 1.12 mW/cm². Upper right: the glass transitions of the partially cured samples (heating rate 10 K/min).

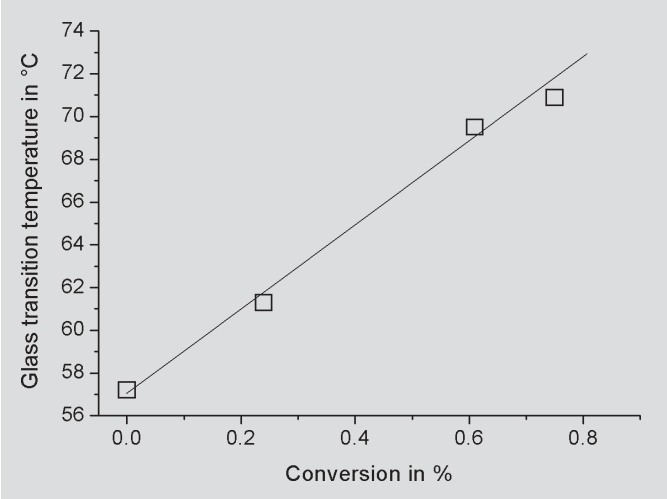


Fig. 11. Glass transition temperature as a function of conversion or degree of cure.

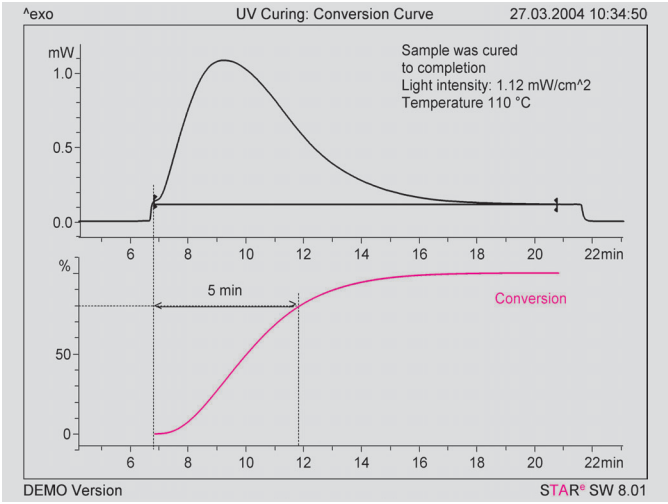


Fig. 12. The UV exposure time necessary to achieve a given conversion or degree of cure, e.g. of 80%, can be determined from the curing curve of a sample that is exposed to UV light until it is fully cured.

UV-DSC experiments showed that about 5 minutes were needed to attain an adequate degree of cross-linking at this temperature and with a light intensity of 1.12 mW/cm$^2$. If the UV light intensity is doubled, the exposure time is reduced to about 3 minutes. There is however a limit to the possible reduction in UV exposure time: light intensities that are too high lead to incomplete curing of the powder coating. On the other hand, UV exposure times that are too long lead to an increase in temperature on the surface of the substrate. This inevitably results in the coating having poorer mechanical properties.

# Quality assurance of plastic molded parts by DSC Part 1: Incoming materials

*Dr. Achim Frick, Claudia Stern, Fachhochschule Aalen, Kunststofftechnik, Aalen, Germany*

The article describes several practical applications that illustrate the use of DSC for the quality control of plastic molded parts. It explains how DSC can be used to identify materials and detect differences between batches. The influence of additives such as colorants and stabilizers is also discussed.

## Introduction

The quality of incoming plastic molding materials is often only assessed by characterizing their flow properties in the melt or in solution, in particular by measuring the melt flow index (MFI) or the viscosity index (VI) in solution. These rheological methods do not however identify the material or allow information to be obtained about melting and solidification behavior, although the latter is directly relevant to the properties of the molded parts produced. This article discusses different applications of DSC for the quality control of incoming materials using practical examples.
Part 2 of this series will deal with the use of DSC for process and production control.

## Material identification

Semicrystalline polymeric materials melt over a temperature range characteristic of the particular type of polymer concerned whereas amorphous molding materials usually exhibit a pronounced glass transition. For this reason, melting temperatures are used to identify semicrystalline thermoplastic molding materials, and glass transition temperatures amorphous materials.

Figure 1 shows the DSC second heating curves of several different polymers. Prior to each measurement, the sample was first heated to eliminate the possible effects of thermal and mechanical history and then cooled reproducibly under control. The melting temperature is taken to be the maximum of the melting peak.

DSC can also distinguish between different variations within a particular class of polymers. This is illustrated in Figure 2, which shows the melting behavior of a POM (polyoxymethylene) homopolymer and a POM copolymer. While the molecules of the homopolymer consist of just one type of monomer, the molecules of the copolymer contain different monomers. These

differences in molecular structure influence the melting behavior of the materials. In this particular case, the melting temperature of the copolymer is about 10 K lower than that of the homopolymer.

## Differences between batches

Plastic molding materials are usually produced in batches. Individual batches may differ because of variations in the polymer synthesis and in compounding. Such difference can be measured by DSC and evaluated. For example, Figure 3 shows the DSC heating and cooling curves of three different batches of the same standard type of POM (POM black). Significant differences in crystallization behavior can be seen in the cooling curves, particularly in the width and temperature maximum of the crystallization peaks. Under defined cooling conditions, different morphological structures are formed when the polymer melt solidifies. This influences the properties of the individual molded parts. Applied to the field of plastics processing, this means that the functional properties of the molded parts can differ due to differences in the materials from batch to batch even though the same processing conditions were used in production. The properties of the parts with respect to quality may therefore also be different.

## Stabilizers

Raw polymers are stabilized to prevent thermal and oxidative aging. In the DSC method, the effect of the stabilizer is assessed by measuring the sample in an oxidative atmosphere (oxygen or air as purge gas). In particular, the beginning of the thermal oxidative degradation of the polymer is measured. Figure 4 shows the behavior of four polypropylene (PP) samples containing different concentrations of thermostabilizers. The decomposition of the PP sample without stabilizer begins immediately after melting is completed. With larger stabilizer contents, the onset of decomposition is shifted to higher temperatures. A stabilizer content of 2% or more ensures that the molding material is adequately stabilized with regard to aging. A closer examination of the curves shows the presence of a small peak at 116 °C.

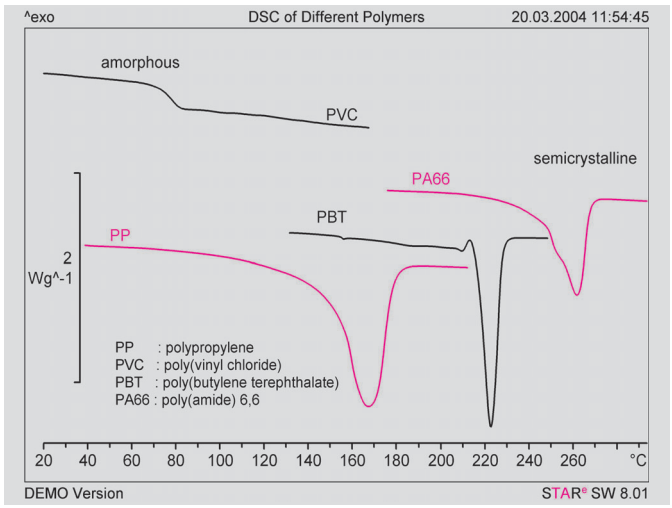


Fig. 1. DSC heating curves (second measurement) of several different polymers: granules; heating rate 20 K/min; purge gas $N_2$.

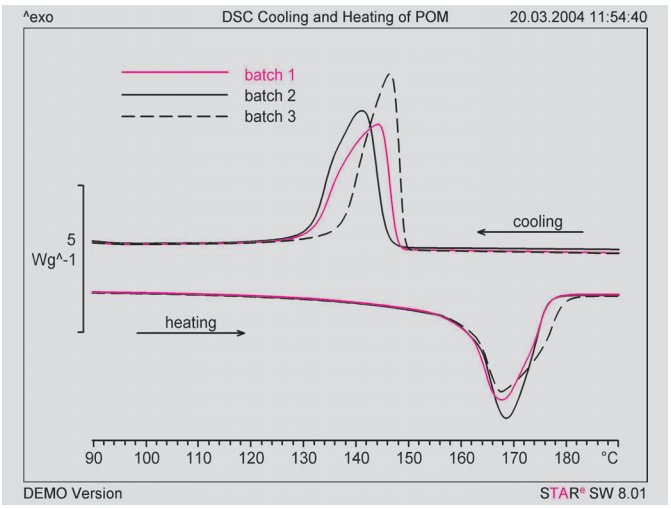


Fig. 3. Cooling curves followed by (second) heating curves of different batches of POM (Hostaform C13021 black). Cooling and heating rates 20 K/min; purge gas $N_2$; sample weight 5.0 ± 0.1 mg).

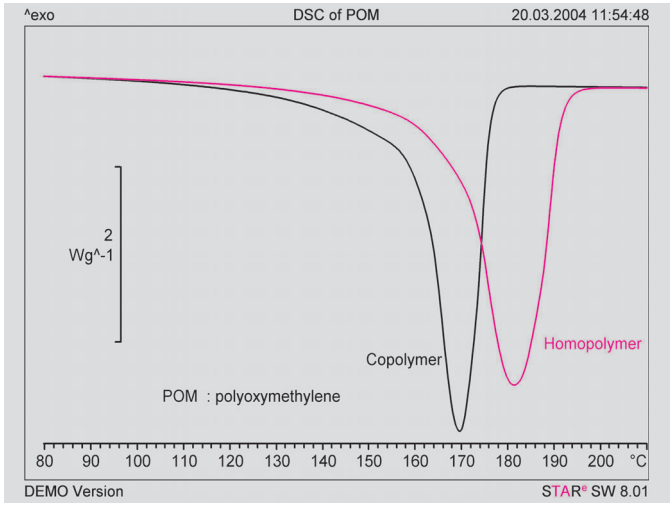


Fig. 2. Melting curves of samples of original POM homopolymer (Delrin 500 CL natur) and original POM copolymer (Hostaform C13021 natur). Heating rate 20 K/min; purge gas $N_2$; sample weight 5.0 ± 0.1 mg.

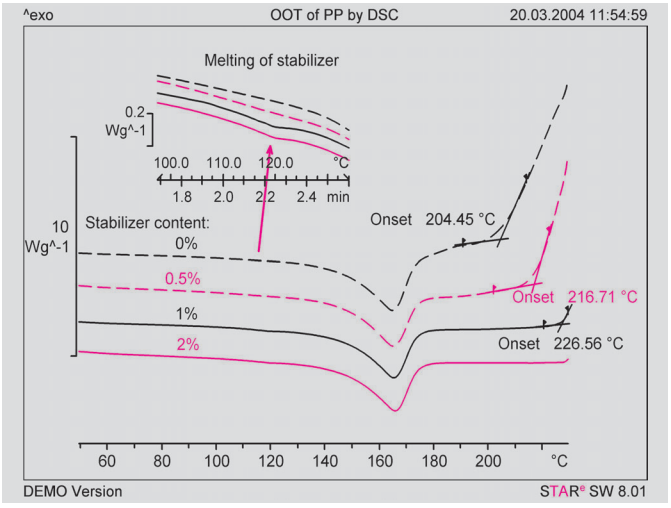


Fig. 4. Oxidation Onset Temperature (OOT) of PP containing different amounts of stabilizer. The inserted diagram displays the melting region of the stabilizer on an expanded scale. Heating rate 20 K/min; purge gas $O_2$; sample weight 5.7 ± 0.1 mg.

This can be assigned to the melting of the thermostabilizer. The peak is displayed on an expanded scale in the inserted diagram in Figure 4.

## Color

Colored molded parts are manufactured either from bulk-colored molding material or by adding a standard color concentrate, a so-called color masterbatch, to the original uncolored molding material. The base material of such color masterbatches is usually a resin formulation or a polyolefine. Processing and technical problems can arise if the melting range of the masterbatch and that of the molding material to be colored are too far apart. To obtain molded parts with optimum properties, e.g. excellent visual homogeneity and processibility, masterbatches based on a polymer matrix should be used for coloring the molding material. The polymer matrix must be compatible with the molding material and melt in the same temperature range otherwise problems arise when the molding material is processed.

DSC measurements can be used to characterize the masterbatch and to estimate the temperature range for processing the molding material. Figure 5 shows the melting curves of a reinforced PP molding material and the color masterbatch. The masterbatch has already completely melted by 118 °C, while the PP molding material only just begins to melt at this temperature. The melting temperatures in fact differ by 48 K, which can lead to processing problems. The melting peak temperature of 117 °C for the granulated coloring material is typical for a color masterbatch. Carbon black is often used to render materials black. Figure 5 shows the DSC curves of unreinforced polybutylene terephthalate (PBT) molding material with and without carbon black. On cooling, the black molding material crystallizes with a peak maximum at 189 °C, whereas the original uncolored molding material has a maximum at 167 °C. The reason for this is the increased crystallization rate due to the effect of the carbon black particles acting as centers for nucleation. This leads to a finer crystalline structure and results in plastic molded parts whose properties are different to those formed from the uncolored polymer melt under the same cooling conditions. The difference in structure is also the reason for the difference in melting behavior. The second heating run of the black sample exhibits two peaks with the first maximum at about 212 °C. This relatively low melting temperature indicates that small crystallites are formed due to the large number of nucleation centers.

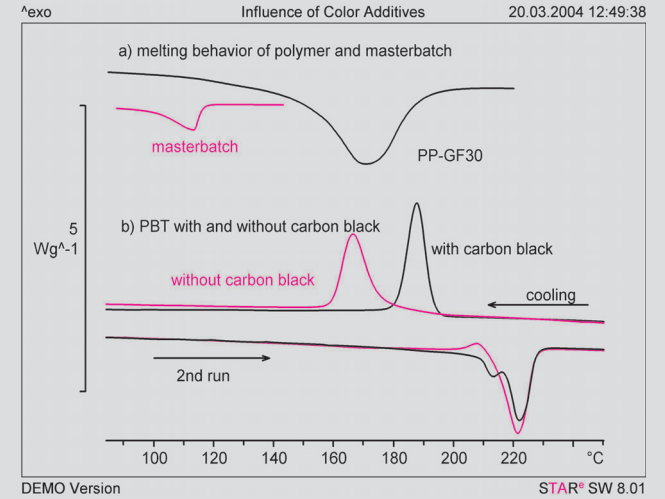


Fig. 5: DSC curves (second heating runs) of differently colored molding materials: a) melting curve of the PP-GF30 polymer and the color masterbatch; b) cooling and second heating curves of differently colored PBT, Ultradur B4520. Heating/cooling rate 20 K/min; purge gas $N_2$; sample weight 3.5 ± 0.1 mg).

## Conclusions

DSC is an excellent method for the quality control and characterization of incoming materials. The analysis of glass transitions, melting and crystallization processes, and chemical reactions provides important information on the identity and stability of the molding materials as well as the influence of different types of additives.

Comprehensive information on the sample preparation and application possibilities of DSC in plastics technology is given in the DSC technical manual. This book can be obtained from Prof. Dr.-Ing. Achim Frick at the Fachhochschule Aalen.

# Dates

### Exhibitions, Conferences and Seminars - Veranstaltungen, Konferenzen und Seminare

| | | |
|---|---|---|
| AIMAT | June 29-July 2, 2004 | Ancona (Italy) |
| Calorimetry & Thermal Effects in Catalysis | July 6-9, 2004 | Lyon (France) |
| 5th International Conf. on Polymer-solvent Complexes & Intercalates | July 11-13, 2004 | Lorient (France) |
| SLAP 2004 | July 11-16, 2004 | Valencia (Spain) |
| ACS | August 23-25, 2004 | Philadelphia, Pennsylvania, (USA) |
| ICTAC | September 12-19, 2004 | Chia Laguna, Sardinia (Italy) |
| NATAS | October 4-6, 2004 | Williamsburg, Virginia, (USA) |
| Het Instrument 2004 | November 1-5, 2004 | Utrecht (Netherlands) |

### TA Customer Courses and Seminars in Switzerland - Information and Course Registration:
### TA-Kundenkurse und Seminare in der Schweiz - Auskunft und Anmeldung bei:

Frau Esther Andreato, Mettler-Toledo, Analytical, Schwerzenbach, Tel: ++41 1 806 73 57, Fax: ++41 1 806 72 40, e-mail: esther.andreato@mt.com

### Courses / Kurse

| | | | |
|---|---|---|---|
| TMA/DMA Basic/SW Basic (Deutsch) | 20. September, 2004 | TMA/DMA Basic/SW Basic (English) | September 27, 2004 |
| TGA/DMA Advanced (Deutsch) | 21. September, 2004 | TGA/DMA Advanced (English) | September 28, 2004 |
| DSC Basic (Deutsch) | 22. September, 2004 | DSC Basic (English) | September 29, 2004 |
| DSC Advanced (Deutsch) | 23. September, 2004 | DSC Advanced (English) | September 30, 2004 |
| SW Advanced (Deutsch) | 24. September, 2004 | SW Advanced (English) | October 1, 2004 |

### TA-Kundenkurse und Seminare in Deutschland

Für nähere Informationen wenden Sie sich bitte an: Frau Inga Kuhn, Mettler-Toledo GmbH, Giessen, Tel: ++49 641 507 404, e-mail: inga.kuhn@mt.com

| | | |
|---|---|---|
| Fachseminar TA-Methoden/Kunststoffe | 22.06.2004 | Frankfurt/M. |
| Fachseminar TA-Methoden/Pharma | 24.06.2004 | München |
| Fachseminar „Dynamisch Mechanische Analyse – die Zukunft für innovative Materialentwicklung» | 01.07.2004 | Frankfurt/M. |
| Branchenworkshop „TA-Methoden in der Pharmazeutik» | 14/15.10. 2004 | Giessen |
| Branchenworkshop «TA&IR an Kunststoffen» | 20/21.10.2004 | Giessen |

Weitere Informationen zu diesen Veranstaltungen finden Sei unter: www.labtalk.de

### TA-Kundenkurse und Informationstage in Österreich

Anmeldung und nähere Informationen: Frau Geraldine Braun, Tel. +43-1-604 19 80 - 48, e-mail: geraldine.braun@mt.com

### TA Semináre v Ceské Republice

Pro blizsí informace prosím kontaktujte: Helena Beránková, Mettler-Toledo Praha, Tel: +420 272 123 152, e-mail: helena.berankova@mt.com

### TA szemináriumok Magyarországon

Részletekkel kapcsolatban szívesen adunk tájékoztatást a Mettler-Toledo magyarországi irodájában.
Tel: +36 1 288-4040, Fax: +36 1 288-4050, e-mail: ilona.matus@mt.com

### Cours et séminaires d'Analyse Thermique en France

Renseignements et inscriptions par
Christine Fauvarque, Mettler-Toledo S.A., 18-20 Av. de la pépinière, 78222 Viroflay Cedex, Tél: ++33 1 3097 1439, Fax: ++33 1 3097 1660

### Cours clients (2ème session)

| | | | | |
|---|---|---|---|---|
| DMA/TMA et le logiciel STARe | 4 octobre 2004 | Viroflay (France) | TGA et logiciel STARe | 7 octobre 2004 Viroflay (France) |
| DSC les bases et logiciel STARe | 5 octobre 2004 | Viroflay (France) | Logiciel STARe | 8 octobre 2004 Viroflay (France) |
| DSC avancé et logiciel STARe | 6 octobre 2004 | Viroflay (France) | | |

### Seminars for Thermal Analysis in Belgium

For more details, please contact Philippe Larbanois, N.V. Mettler-Toledo S.A., Zaventem, Tél: ++32 2 334 02 11, Fax: ++32 2 334 03 34.
e-mail: philippe.larbanois@mt.com

### TA Customer Courses and Seminars in the Netherlands

Voor verdere informatie kunt U kontakt opnemen met: Hay Berden of Ko Schaap, Mettler-Toledo B.V., Tiel, Tel: ++31 344 63 83 63

### Corsi e Seminari di Analisi Termica in Italia

Per ulteriori informazioni Vi preghiamo di contattare:
Marina Varallo, Mettler-Toledo S.p.A., Novate Milanese, Tel: ++39 02 333 321, Fax: ++39 02 356 2973, e-mail: marina.varallo@mt.com

| | | | |
|---|---|---|---|
| DSC base | 28 Settembre 2004 Novate Milanese | TGA | 30 Settembre 2004 Novate Milanese |
| DSC avanzato | 29 Settembre 2004 Novate Milanese | TMA | 1 Ottobre 2004 Novate Milanese |

### Cursos y Seminarios de TA en España

Para detalles acerca de los cursos y seminarios, por favor, contacte con:
Francesc Catala, Mettler-Toledo S.A.E., Tel: ++34 93 223 76 00, e-mail: francesc.catala@mt.com

| | | | |
|---|---|---|---|
| Seminario de aplicaciones TA: | Septiembre 21, 2004 Madrid | Seminario de aplicaciones TA: | Septiembre 28, 2004 Barcelona |
| Seminario para usuarios STARe: | Septiembre 22, 2004 Madrid | Seminario para usuarios STARe: | Septiembre 29, 2004 Barcelona |

### TA Customer Courses and Seminars for Sweden and the Nordic countries

For details of training courses and seminars, please contact:
Fredrik Einarsson, Mettler-Toledo AB, Tel: ++46 455 30 0080, Fax: ++46 8 642 45 62, e-mail: fredrik.einarsson@mt.com

### TA Customer Courses and Seminars in the UK

For details of training courses and seminars, please contact:
Rod Bottom, Mettler-Toledo Ltd, Leicester, Tel: ++44 116 234 5025, Fax: ++44 116 236 5500

| | | | |
|---|---|---|---|
| DSC Basic | 26 October, 2004 Leicester | DSC Basic | 27 October, 2004 Leicester |

### TA Customer Courses and Seminars in the USA and Canada

Basic Thermal Analysis Training based on the STARe System is being offered at various locations.
For information, please contact: Tom Basalik at +1 614 438 4687, Fax: +1 614 438 4693 or by e-mail to: tom.basalik@mt.com

| | | | |
|---|---|---|---|
| Curve Interpretation | September 2, 2004 Blue Ash, OH | Curve Interpretation | September 29, 2004 Durham, NC |
| Sample Preparation | September 2, 2004 Blue Ash, OH | Sample Preparation | September 29, 2004 Durham, NC |
| STARe User Training | September 21-22, 2004 Columbus, OH | Automotive Analysis by DMA | October 20, 2004 Southfield, MI |
| | | Sample Preparation | October 20, 2004 Southfield, MI |

### TA Customer Courses in the South East Asia Regional Office, Kuala Lumpur

For information on dates, please contact:
Malaysia: Ricky Tan at ++603 78455773, Fax: 603 78458773
Singapore: Joslyn Yeo at ++65 8900011, Fax: 65 8900013
Thailand: W. Techakasembundit at ++662 7230336, Fax: 662 7196479
or SEA regional office: Soosay P. at ++603 78455373, Fax: 603 78453478

### TA Seminars in Taiwan

For details of seminars please contact: Kimmy Wu at Mettler-Toledo Taiwan, Tel: ++886 2 6578898, Fax: ++886 2 26570776,
e-mail to kimmy.wu@mt.com and visit our home page at http://www.tw.mt.com

### TA Customer Courses and Seminars in Japan

For details of training courses and seminars please contact:
Yasushi Ikeda at Mettler-Toledo Japan, Tel: ++81 3 5762 0746, Fax: ++81 3 5762 0758, or by e-mail to yasushi.ikeda@mt.com

| | | | |
|---|---|---|---|
| TA/FP Workshop | August 3, 2004 Tokyo Service Center | TA/FP Workshop | August 5, 2004 Osaka Service Center |
| Infoday Seminar | October 19, 2004 Tokyo Technical Center | Infoday Seminar | October 21, 2004 Osaka Branch |

### Cursos y Seminarios de TA en Latin America

Para detalles acerca de los cursos y seminarios, por favor, contacte con:
Francesc Català, Mettler-Toledo, LA, Tel: ++34-932 237 615 (Spain), e-mail: francesc.catala@mt.com

### Editorial team


Dr. J. Schawe, Physicist


Dr. R. Riesen, Chem. Engineer


J. Widmann, Chem. Engineer


Dr. M. Schubnell, Physicist


C. Darribère, Chem. Engineer


Dr. M. Wagner, Chemist


Dr. D. P. May, Chemist


Ni Jing, Chemist


Urs Jörimann, Electr. Engineer

METTLER-TOLEDO GmbH, Analytical, Sonnenbergstrasse 74, CH-8603 Schwerzenbach, Switzerland
Kontakt: urs.joerimann@mt.com, Tel: ++41 1 806 73 87, Fax: ++41 1 806 72 60
Internet: http:/www.mt.com/ta